Effect of Nasal High Flow Therapy on CO_2 Tension - Physico-mathematical Modelling

[1] Cletus F. Adams, [2] Mark Jermy ,[3] P. H. Geoghegan

Centre for Bioengineering
Dept. of Mechanical Engineering
University of Canterbury
New Zealand
email: [1] cleadams.23@gmail.com
[2] mark.jermy@canterbury.ac.nz
[3] patrick.geoghegan@canterbury.ac.nz

C. J. T. Spence

Fisher & Paykel Healthcare
Auckland, New Zealand
email: Callum.Spence@fphcare.co.nz

***Abstract*—The respiratory system of a human embodies complex assembly of tissues and organs (typically internal and external intercostal muscles, diaphragm, lung and rib cage), which are coordinated in a fashion that allows the influx and efflux of air into the airways and lungs. Like all other biological systems, the respiratory system is susceptible to injuries and diseases. Where ventilation has been severely impaired leading to poor gaseous exchange across the lung tissue, biomechanical therapeutic modalities such as continuous positive airway pressure (CPAP) and mechanical ventilators have been prescribed for such patients. Currently, Nasal High Flow therapy (NHFT), a novel ventilation technique has been reported to improve gaseous exchange in both neonates and adults by supplying a constant flow of humidified and warmed air into the lungs. NHFT is presently applied in the management of apnoea of prematurity, respiratory distress syndrome, bronchiolitis, and acute lung injury. In spite of reported success, its mechanisms of action (MOA) are not wholly understood. This work, in terms of relevance, provides some insights into the MOA of NHFT by underscoring the mathematical basis for reported improved gaseous exchange during the administration of NHFT. The mathematical model predictions appreciably agreed with bench-top measurements - indicating 17 % and 24% reduction in end tidal CO_2 concentration upon the respective administration of 30 l/min and 60 l/min NHFT.**

Keywords–nasal high flow therapy; capnography; dead space; alveolar CO_2 tension.

I. INTRODUCTION

Capnography is the process of analysing the partial pressure of CO_2 in respiratory gases [1]. Owing to the importance of capnography in current medical practice, medical bodies including the American Association for Respiratory Care [1] and American Society of Anesthesiologists [2] [3] have endorsed it as a method for verifying the correct placement of endotracheal tubes for the provision of respiratory support. Where blood acidosis is clinically diagnosed, capnography may be used to identify the cause by checking for hypercarbia ($PaCO_2 > 45$ mmHg) [4]. Additionally, since CO_2 is transported from the cells (sites of metabolism) to the lungs via the circulatory system, events such as pulmonary and vascular embolism can be detected using capnography [5].

The CO_2 profile recorded during a breathing cycle is unique in terms of morphology for healthy individuals [6][2]. A CO_2 tension profile for a healthy state is shown in Figure 1. Phase I denotes the baseline where inspiration is about to end. The transition stage, Phase II, physically represents a blending of alveolar CO_2-rich air and dead space air. Phase III (alveolar plateau) indicates an almost complete saturation of the airway with alveolar air and peaks at point E_tCO_2, known as end-tidal concentration of CO_2 . Inspiration begins immediately after E_tCO_2 - marking the commencement of phase IV, where influx of fresh atmospheric air speedily dilutes airway air until the baseline value is reached [6][5][7]. Essentially, deviations from healthy state morphology may be suggestive of a pathological condition of the respiratory system [7][3]. It has been mentioned that changes in baseline level, steadiness of the alveolar plateau and slope of transitional portion may be cardinal to the clinical diagnosis of CO_2 rebreathing and pneumothorax [3][5].

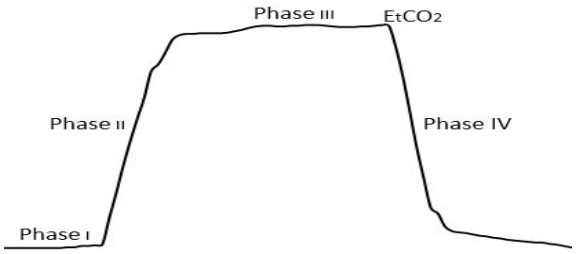

Figure 1. Morphology of a healthy adult capnogram.

Figure 2 shows two polymer models of the upper airway geometry fabricated for experimental work. To fabricate this, a set of computer tomography (CT) images obtained from an adult (age = 44 years and gender = male) was used to reconstruct an *in silico* anatomically representative 3-D model of the upper airway. A detailed description of model making methods has been outlined by Geoghegan et al. [8]. A physical upper airway model, patterned according to the *in silico* model, was built by the use a 3-D printer (fused deposition modelling type), which utilized acrylonitrile butadiene styrene (ABS) as print material.

Nasal high flow therapy (NHFT) involves the administration of humidified and heated air (up to normothermia) at a constant flow rate. Figure 3 is a pictorial representation of the administration of NHFT via a nasal cannula using Fisher & Paykel Healthcare Airvo2 device. It has been reported that NHFT washes the nasopharygeal dead space resulting in an increased proportion of inhaled oxygen content and

 ISBN: 978-1-61208-488-6

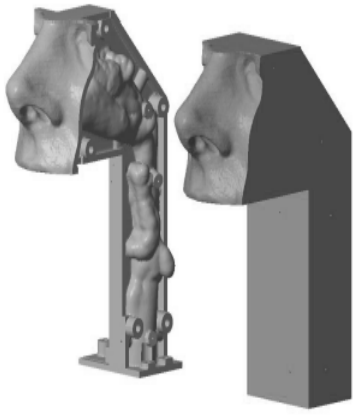

Figure 2. Polymer model of upper airway.

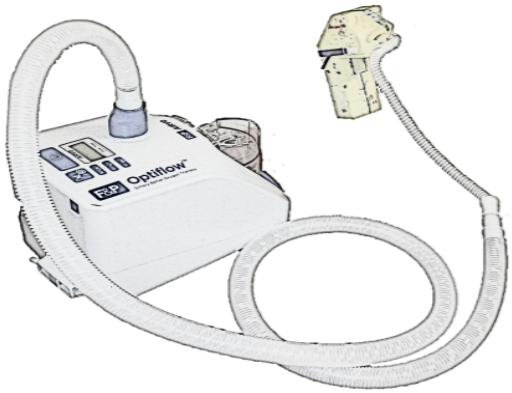

Figure 3. Setup for NHFT administration.

a subsequent improvement in gaseous exchange across the blood-gas barrier [9][10][11]. Arthur et al. [12] pioneered the use of physico-mathematical models to investigate CO_2 fluctuations in the pulmonary system. Their analysis explained the effect of rebreathing on pulmonary CO_2 tension profile. Authors such as Finchman et al. [13] and Milhorn et al [14] used sophisticated compartmental models which included homeostatic response mechanisms, to provide insight into arterial and alveolar reactions to step changes in inhaled CO_2 amounts. Quite recently, Swanson et al. [15] and Benallal et al. [16] applied a two compartment model to shed light on alveolar gas changes during exercise. In the present work, an identical two compartment model has been modified to investigate the amount of CO_2 flushing from the dead space under the influence of NHFT.

In Section 2, formulation of the mathematical model along with the experimental setup is presented. Section 3 comprises of results obtained from both mathematical simulation and bench-top experiment. A discussion of results and concluding observations are presented in Sections 4 and 5 respectively.

II. METHOD

A. Modelling setup

The model presented in this work is identical to that used by Benallal et al. [16] however the inclusion of a constant volumetric flow term to cater for NHFT distinguishes the present model (Figure 4) from it. In this model, the volume of the respiratory system has been thought of as compartmentalized into two main units, namely dead space unit and alveolar unit. The dead space unit represents the volume of all airway regions where gaseous exchange does not occur whilst the alveolar unit denotes the combined volume of lung and airway regions that exchange gas with pulmonary capillaries. Assumptions made during the formulation of model equations include the following (a) administration of NHFT does not change the dead space volume (time invariant) (b) alveolar volume changes due to NHFT is insignificant (c) there is negligible gas loss across the walls of the dead space.

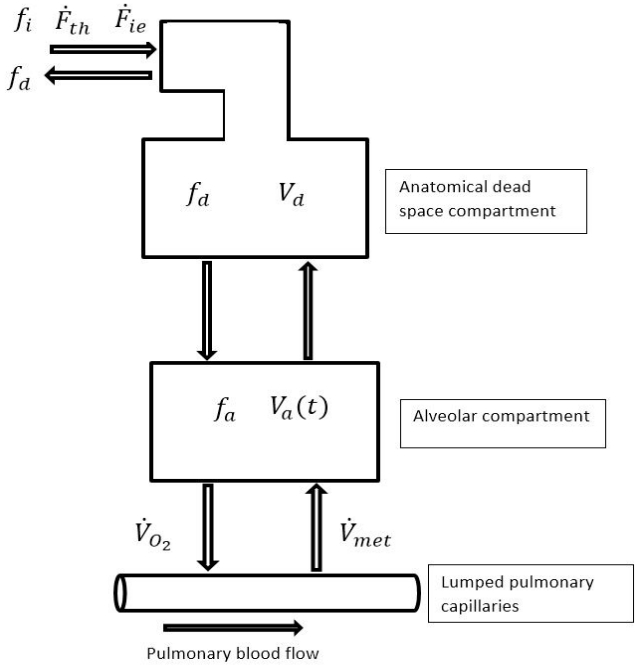

Figure 4. Model representation of respiratory system.

A description of the symbols used in Figure 4 and model equations (1-5) is presented in Table I. Tidal flow data of a healthy male adult (age 23, BMI = 24.6), acquired using a spirometer setup, was used as an input signal to the model. The flow signal was scaled to produce a tidal volume of 500 ml, which is the estimated average for healthy adults [17]. For a resting phase spontaneous breathing of an adult, the functional residual capacity, average metabolic CO_2 production rate ($\dot{V}_{met}$) and O_2 exchange rate ($\dot{V}O_2$) across the blood gas barrier were specified as 2500 ml, 240 ml/min and 300 ml/min respectively as used by several authors [16][15][14][5]. Equations (1) and (2) are descriptive of the CO_2 balance in the dead space unit during inspiration and expiration, respectively. In a like manner, the material balance of CO_2 in the alveolar compartment during the breathing cycle is represented by (4) and (5). The alveolar volumetric transience is described by

equation 3. In equations 1, 2, 4 and 5, $\dot{V}_{ie} = \dot{F}_{th} + \dot{F}_i e$.

To solve this 5 non-linear system of equations, a Runge-Kutta (4,5) based solver, ode45, custom-packaged in Matlab (Version 2014b) was employed. The simulation was performed using 50 breathing cycles, which is equivalent to 3.5 minutes of breathing.

TABLE I. MODEL AND EQUATION PARAMETERS.

Symbol	*Parameter*	*Value*
f_d	dead space CO_2 fraction	-
f_a	alveolar CO_2 fraction	-
$\dot{F}_{ie}$	ventilatory flow	-
$\dot{F}_{th}$	NHFT flow	30 and 60 l/min
f_i	inspiratory CO_2 fraction	-
V_a	alveolar volume (time variant)	-
V_d	dead space volume (constant)	150 ml
$\dot{V}_{met}$	metabolic CO_2 influx	240 ml/min
$\dot{V}O_2$	O_2 exchange rate	300 ml/min

$$\frac{df_dCO_2}{dt} = \frac{(\dot{V}_{ie})(f_i - f_d)}{V_d} \quad (1)$$

$$\frac{df_dCO_2}{dt} = \frac{\dot{V}_i e(f_a - f_d)}{V_d} \quad (2)$$

$$\frac{dV_a}{dt} = \dot{V}_{ie} + \dot{V}_{met} - \dot{V}0_2 \quad (3)$$

$$\frac{df_aCO_2}{dt} = \frac{\dot{V}_{ie}f_d + \dot{V}_{met} - f_a(\dot{V}_{ie} + \dot{V}_{met} - \dot{V}O_2)}{V_a} \quad (4)$$

$$\frac{df_aCO_2}{dt} = \frac{\dot{V}_{met} - f_a\dot{V}_{ie} + f_a(\dot{V}_{ie} + \dot{V}_{met} - \dot{V}O_2)}{V_a} \quad (5)$$

A sensitivity study was performed to evaluate the independent contribution of the model parameters to E_tCO_2. The resolution of the sensitivity scale was limited to a 1 % change in E_tCO_2 because a 1 % change significantly affects amount of CO_2 flushed when NHFT is applied. Findings for a 10 % increment on each parameter value is presented in Table II. E_tCO_2 was found to be most responsive to initial value of alveolar CO_2 partial pressure ($PACO_2$) and metabolic CO_2 production rate. Variation in initial dead space CO_2 fraction produced the least change in E_tCO_2.

TABLE II. SENSITIVITY STUDY.

Parameter	*10% value increment*	Change in E_tCO_2	*Comment*
initial $PACO_2$	5.86 %	7.71%	very sensitive
$\dot{V}_{met}$	275 ml	1.06 %	sensitive
initial f_i	0.048 %	0.05 %	less sensitive
FRC	2750 ml	0.12 %	less sensitive
V_d	165 ml	0.43 %	less sensitive
$\dot{V}O_2$	330 ml/min	0.15%	less sensitive

B. Experimental work

The same physiological flow signal as specified for the mathematical model was programmed into a LabVIEW (Version 8.6) application that operates a pulsatile pump (Figure 5). See component labelling of Figure 5 for setup description. The pulsatile pump (2) connects to a 3-D printed upper airway model via a tubing. NHFT is administered through a nasal cannula (4) by means of a Fisher & Paykel Airvo2 device (3). In performing CO_2 experiments, CO_2 was metered at a bleed rate of 250 ml/min into the pump chamber (piston barrel) , allowing a back pressure of 101.3 KPa in the CO_2 source (1). Measurement of CO_2 concentration at the trachea opening of the airway model is performed using a capnograph (5). After a minute, a steady CO_2 profile peaking at E_tCO_2 of 5.2% was observed on the computer (6) connected t the capnograph.

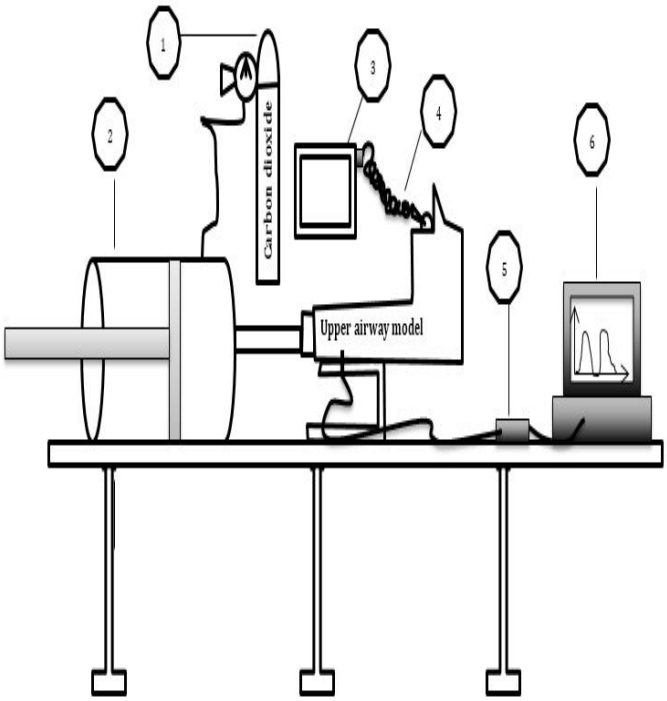

Figure 5. Complete experimental setup

At this point, recording of CO_2 data was performed for 3 minutes followed by 30 l/min NHFT - administered using Fisher & Paykel Healthcare Airvo2 device. Two minutes was allowed for equilibration after which CO_2 recording proceeded for 3 more minutes. An identical procedure was repeated for 60 l/min NHFT, after residual effects from the previous experiment had been eliminated by shutting off CO_2 bleed valve whilst the pump was in operation - allowing CO_2 levels to plummet to near atmospheric values.

III. RESULTS

On Figure 6, plot A shows fractional CO_2 profile in the alveolar unit during a 50 breathing cycle simulation. Transience in breath-by-breath CO_2 fraction is observable up to 60 seconds and then a steady state is reached. The

flow wave used for both simulation and experiment had a period of 4.3 seconds - inspiratory time being 2 seconds and expiratory time being 2.3 seconds. Plot B (Figure 6) represents two cycles of zero-therapy (ZT) ventilatory flow patterns superimposed on corresponding alveolar CO_2 fraction profile at steady state. The distortions on the flow wave at the interface between inspiration and expiration are artefacts introduced by the limited resolution of the spirometer flow device, which is directly linked to the observable local perturbations in fractional alveolar CO_2 profile at the flow transition points. The alveolar CO_2 fraction is seen to rise up to 0.3 seconds into inspiration. Furthermore, over the respiratory cycle, alveolar CO_2 fraction fluctuates between 4.9 % and 5.3 % with a mean value corresponding to 5.1 % .

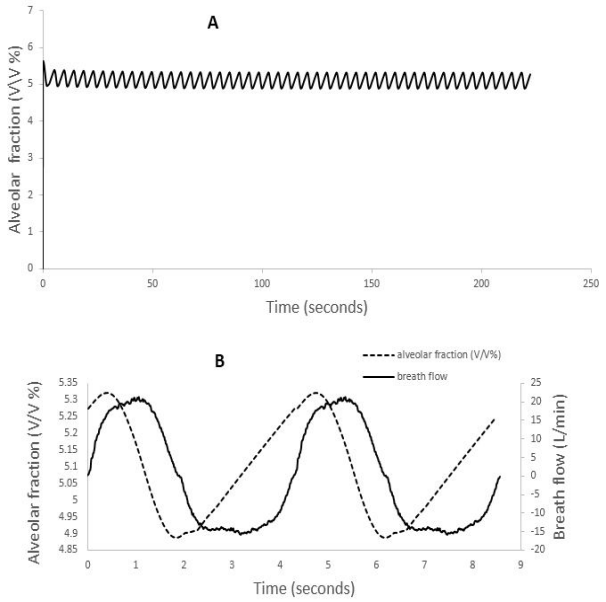

Figure 6. Variation of alveolar CO_2 tension with time.

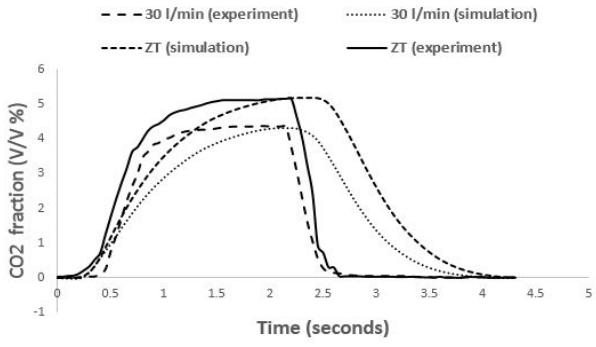

Figure 7. Variation of deadspace CO_2 tension with time.

Figure 7 shows a single respiratory cycle plot of experimental and simulated dead space CO_2 fraction profiles for both ZT and 30 l/min NHFT conditions. When 30 l/min NHFT was applied , dead space E_tCO_2 fell from 5.2 % to about 4.3 % (17% decrement). It is observable from Figure 8 that for 60 l/min NHFT, model simulation under predicts experimental E_tCO_2 by a margin of 8%. In morphology,

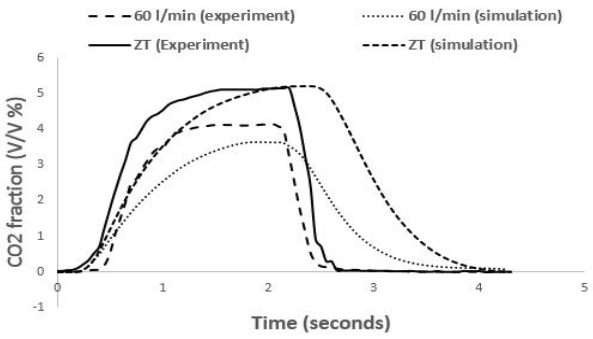

Figure 8. Variation of deadspace CO_2 tension with time.

the simulated dead space CO_2 fraction does not match very well with the experimental measurements. This may be due to the inherent perfect mixing of CO_2 in the dead space compartment (not realistic) which can be made physiological by sub-dividing the dead space volume into several control volumes. The area under the plots (Figures 7 and 8) contain information about dead space CO_2 volume. In quantitative terms, mathematical simulation over-predicts the combined inspiratory and expiratory CO_2 volume for both ZT and 30 l/min NHFT by 8 %. On the same note, CO_2 volume over the respiratory cycle for 60 l/min NHFT is over-predicted by 4%.

IV. Discussion

Generally, the pulsatile pump setup differs from *in vivo* conditions in two aspects, i.e., compliance mismatch (high rigidity of piston barrel) and absence of O_2 exchange mechanism. Since lung elasticity does not enter into the model equations (1-5) and the pulsatile pump is able to deliver the expected tidal volume, the influence of tissue elasticity is eliminated. Given that the ratio of exchanged O_2 volume to tidal volume is quite small (1:25), the present experimental results may therefore considerably approximate the results for the case where an O_2 absorption unit is included in the pulsatile pump assembly. Simulation of no-oxygen condition, however, has indicated a 5 % reduction in expired CO_2 volume.

E_tCO_2 obtained via simulation is comparable to corresponding experimental values for ZT and 30 l/min NHFT. For all cases, slopes of capnogram phases II and IV as predicted by simulation are lesser compared to experimental observations (Figures 7 and 8). This may be due to the model compartmental configuration, which allows for full CO_2 mixing at all times whilst in the experimental setup (same as *in vivo*) there is an established CO_2 front which takes a finite time to travel along the airway. For 60 l/min NHFT, the model under-predicts experimental E_tCO_2 by a change of 8 %. This may be considered as a pronounced effect of the afore-mentioned full CO_2 mixing (not physiological), being heightened by high levels of NHFT.

ZT E_tCO_2 of 5.2 % obtained from simulation corresponds to a tension of 38 mmHg . This value is within physiologic range (37 - 44 mmHg) for healthy adults [18]. The mean alveolar CO_2 fraction of 5.1 % is equivalent to alveolar CO_2 tension ($PACO_2$) of 39 mmHg, which agrees with the reported physiologic range of 35 mmHg to 45 mmHg [19][20][21]. The rise in alveolar CO_2 fraction for about 0.3 seconds into inspiration is suggestive of rebreathing of CO_2 from the dead

space unit [12].

Over a spontaneous breathing cycle, mean arterial CO_2 pressure ($PaCO_2$) is approximately the mean of $PACO_2$. It has been reported that the lungs can sufficiently engage in oxygen exchange when it is in the state of apnoea, however in this state, CO_2 diffusing across the blood-gas barrier accumulates in the lung and can potentially cause blood acidosis ($PaCO_2 >$ 45 mmHg). Several studies have mentioned an increase in ventilatory rate in severe COPD patients experiencing hypercapnic events ($PACO_2 > 45$ mmHg), which has been interpreted as a homeostatic reaction to maintain $PACO_2$ in physiological range [14]. The mean $PACO_2$ output from the present model may potentially provide some insights into expected $PaCO_2$ for COPD related hypercapnic events under NHFT conditions. On Figure 7, there is a 17 % fall in E_tCO_2 when 30 liters/min NHFT is applied. The washout volume of CO_2 during expiration, as predicted by the model is 2 ml - representing 15 % of the total expired CO_2 volume for spontaneous breathing. Experimentally, administration of 60 l/min NHFT yielded 24% reduction of ZT E_tCO_2 though the simulated results over-predicts this change. It is however noticeable that the amount of reduction in E_tCO_2 is dependent on flow rate at which NHFT is administered.

Spence et al. [11] used particle imaging velocimetry (PIV) techniques to investigate flow distribution in a silicone upper airway model under NHFT conditions. Their conclusion was that recirculation currents observed in the nasopharynx resulted in CO_2 flushing. Chatila et al. investigated exercise tolerance of severe COPD patients and concluded that NHFT leads to a gain in exercise endurance attributable to increased oxygenation. Flushing of CO_2 may increase the proportion of alveolar ventilation in reference to minute ventilation, thereby boosting oxygen exchange across the blood-gas interface in the lungs [10]. In the light of these reports, the presented two-compartment model , in spite of the outlined limitations, appreciably predicts changes in E_tCO_2 of the bench-top model capnogram for both zero-therapy and NHFT conditions.

V. Conclusion

The results from this work show that it is possible to make appreciably satisfactory predictions of the end tidal CO_2 fraction, alveolar CO_2 tension and flushed CO_2 volume for nasal high flow therapy conditions though in terms of morphology, results from the presented two-compartment model show a width-wise disparity from physiologic CO_2 profiles.

Acknowledgment

The authors would like to thank UC Doctoral Scholarship and Fisher & Paykel Healthcare for their support.

References

[1] B. K. Walsh, D. N. Crotwell, and R. D. Restrepo, "Capnography/Capnometry During Mechanical Ventilation: 2011," *Respiratory Care*, vol. 56, pp. 503–509, Apr. 2011.

[2] M. B. Jaffe, "Volumetric Capnography, The Next Advance in CO2 Monitoring," *Respironics Inc (Critical Care)*, 2006.

[3] J. E. Thompson and M. B. Jaffe, "Capnographic waveforms in the mechanically ventilated patient," *Respiratory care*, vol. 50, no. 1, pp. 100–109, 2005.

[4] H. Soleimanpour, "Capnography in the Emergency Department," *Emergency Medicine: Open Access*, vol. 02, no. 09, 2012.

[5] J. O. Den Buijs, L. Warner, N. W. Chbat, and T. K. Roy, "Bayesian tracking of a nonlinear model of the capnogram," in *Engineering in Medicine and Biology Society, 2006. EMBS'06. 28th Annual International Conference of the IEEE*, pp. 2871–2874, IEEE, 2006.

[6] G. Tusman, A. Scandurra, S. H. Bhm, F. Suarez-Sipmann, and F. Clara, "Model fitting of volumetric capnograms improves calculations of airway dead space and slope of phase III," *Journal of Clinical Monitoring and Computing*, vol. 23, pp. 197–206, Aug. 2009.

[7] B. You, R. Peslin, C. Duvivier, V. D. Vu, and J. P. Grilliat, "Expiratory capnography in asthma: evaluation of various shape indices," *European Respiratory Journal*, vol. 7, no. 2, pp. 318–323, 1994.

[8] P. H. Geoghegan, N. A. Buchmann, C. J. T. Spence, S. Moore, and M. Jermy, "Fabrication of rigid and flexible refractive-index-matched flow phantoms for flow visualisation and optical flow measurements," *Experiments in fluids*, vol. 52, no. 5, pp. 1331–1347, 2012.

[9] S. et al., "Beneficial effects of humidified high flow nasal oxygen in critical care patients: a prospective pilot study," *Intensive care medicine*, vol. 37, no. 11, pp. 1780–1786, 2011.

[10] K. Dysart, T. L. Miller, M. R. Wolfson, and T. H. Shaffer, "Research in high flow therapy: Mechanisms of action," *Respiratory Medicine*, vol. 103, pp. 1400–1405, Oct. 2009.

[11] C. J. T. Spence, N. A. Buchmann, and M. C. Jermy, "Unsteady flow in the nasal cavity with high flow therapy measured by stereoscopic PIV," *Experiments in fluids*, vol. 52, no. 3, pp. 569–579, 2012.

[12] A. B. Chilton and R. W. Stacy, "A mathematical analysis of carbon dioxide respiration in man," *The bulletin of mathematical biophysics*, vol. 14, no. 1, pp. 1–18, 1952.

[13] W. F. Fincham and F. T. Tehrani, "A mathematical model of the human respiratory system," *Journal of biomedical engineering*, vol. 5, no. 2, pp. 125–133, 1983.

[14] H. T. Milhorn, R. Benton, R. Ross, and A. C. Guyton, "A mathematical model of the human respiratory control system," *Biophysical Journal*, vol. 5, no. 1, pp. 27–46, 1965.

[15] G. D. Swanson and D. L. Sherrill, "A model evaluation of estimates of breath-to-breath alveolar gas exchange," *Journal of Applied Physiology*, vol. 55, no. 6, pp. 1936–1941, 1983.

[16] H. Benallal and T. Busso, "Analysis of end-tidal and arterial PCO2 gradients using a breathing model," *European journal of applied physiology*, vol. 83, no. 4-5, pp. 402–408, 2000.

[17] M. P. Hlastala, "A model of fluctuating alveolar gas exchange during the respiratory cycle," *Respiration physiology*, vol. 15, no. 2, pp. 214–232, 1972.

[18] J. Ritchie, A. Williams, C. Gerard, and H. Hockey, "Evaluation of a humidified nasal high-flow oxygen system, using oxygraphy, capnography and measurement of upper airway pressures," *Anesth Intensive Care*, vol. 39, no. 6, pp. 1103–1110, 2011.

[19] E. D. Robin, R. D. Whaley, C. H. Crump, and D. M. Travis, "Alveolar Gas Tensions, Pulmonary Ventilation and Blood pH During Physiologic Sleep in Normal Subjects1," *Journal of Clinical Investigation*, vol. 37, pp. 981–989, July 1958.

[20] J. N. Mills, "Changes in alveolar carbon dioxide tension by night and during sleep," *The Journal of Physiology*, vol. 122, pp. 66–80, Oct. 1953.

[21] C. J. Allen, N. L. Jones, and K. J. Killian, "Alveolar gas exchange during exercise: a single-breath analysis," *Journal of Applied Physiology*, vol. 57, no. 6, pp. 1704–1709, 1984.

 ISBN: 978-1-61208-488-6